

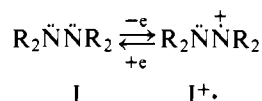
# Geometry Change upon Electron Removal from a Tetraalkylhydrazine. X-ray Crystallographic Structures of 9,9'-Bis-9-azabicyclo[3.3.1]nonane and Its Radical Cation Hexafluorophosphate

S. F. Nelsen,\* W. C. Hollinsed, C. R. Kessel, and J. C. Calabrese

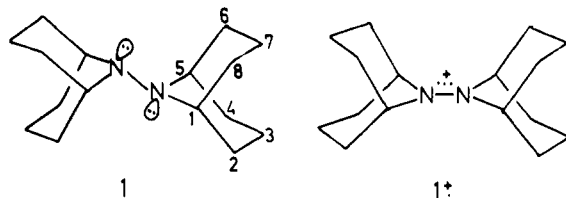
Contribution from the Department of Chemistry, University of Wisconsin, Madison, Wisconsin 53706. Received May 8, 1978

**Abstract:** X-ray crystal structures of 9,9'-bis-9-azabicyclo[3.3.1]nonane (**1**) and its radical cation hexafluorophosphate salt ( $1^+\cdot\text{PF}_6^-$ ) are reported. Crystals of **1** are triclinic  $P\bar{1}$  with  $a = 6.877$  (2) Å,  $b = 6.514$  (2) Å,  $c = 9.380$  (2) Å,  $\alpha = 91.45$  (2)°,  $\beta = 112.74$  (2)°,  $\gamma = 112.82$  (2)°,  $V = 350.0$  (2) Å<sup>3</sup>, and  $Z = 1$ . The structure was solved by direct methods and refined to  $R_1 = 4.0\%$  and  $R_2 = 4.8\%$  for 892 independent reflections. Crystals of  $1^+\cdot\text{PF}_6^-$  ( $-60$  °C) are tetragonal  $P4_2/mmm$  ( $D_{4h}^{14}$ , no. 136) with  $a = b = 7.407$  (2) Å,  $c = 16.629$  (10) Å,  $V = 912.4$  (7) Å<sup>3</sup>, and  $Z = 2$ . Solution of the structure via heavy atom methods and refinement gave  $R_1 = 6.3\%$  and  $R_2 = 8.2\%$  for 524 independent reflections. The NN bond length of  $1^+\cdot\text{PF}_6^-$  is 1.269 (7) Å, surprisingly much shorter than the 1.505 (3) Å for **1**, and the nitrogens of  $1^+\cdot\text{PF}_6^-$  are coplanar with the attached carbons, but those of **1** are bent past tetrahedral ( $\beta = 56.8^\circ$ ).

The tetraalkylhydrazine–tetraalkylhydrazine radical cation electrochemical couple ( $1,1^+\cdot$ ) has been of particular interest to us because of the great change in geometry ex-



pected upon electron removal. Hydrazines are nearly tetrahedral at nitrogen and have an electronic preference for gauche lone pairs,<sup>1</sup> although structural constraints of the alkyl substituents can force the lone pair–lone pair dihedral angle to assume values ranging from 0 to 180°.<sup>2–4</sup>  $1^+$  is isoelectronic with ethylene radical anion, and might be expected to have parallel, p-rich “lone pair” nitrogen orbitals, with an antibonding electron in this NN “ $\pi$ ” system. The parent hydrazine cation radical ( $\text{N}_2\text{H}_4^+\cdot$ ) is essentially planar,<sup>5</sup> and ESR studies of  $1^+$  have indicated that it is also flattened at nitrogen. Specially constrained cases are clearly nonplanar at nitrogen in their equilibrium geometry,<sup>6</sup> and all are easily deformed from planarity at nitrogen. The extensive structural change involved in the  $1,1^+$  couple has been argued to be responsible for the unusually large range of standard oxidation potentials observed<sup>7</sup> and for the unusually low rates for  $1,1^+$  electron transfer. The kinetic stabilization of cationic species having all  $\alpha$  hydrogens constrained to lie in a plane perpendicular to the charge-bearing orbital<sup>9,10</sup> has allowed the chemical oxidation of the title compound **1** to give its hexafluorophosphate salt,  $1^+\cdot\text{PF}_6^-$ , as an isolable, crystalline solid.

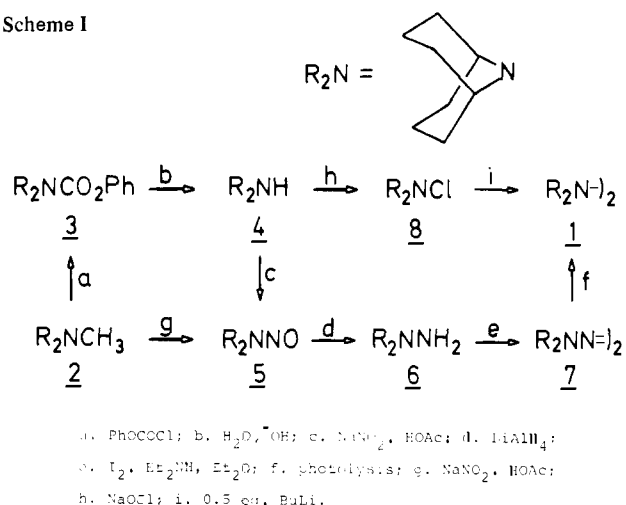


We report here X-ray crystallographic studies of these compounds, which fully document the conformational change upon electron removal which has previously been assumed, and justify the description of  $1^+$  as “olefin-like” in its geometry.

## Compound Preparation

We initially prepared **1** from **2** by reactions a–f,<sup>9</sup> as outlined in Scheme I. It proves to be more convenient to convert *N*-

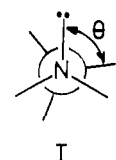
Scheme I

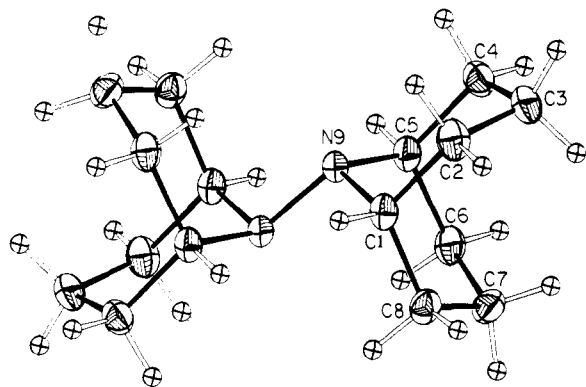
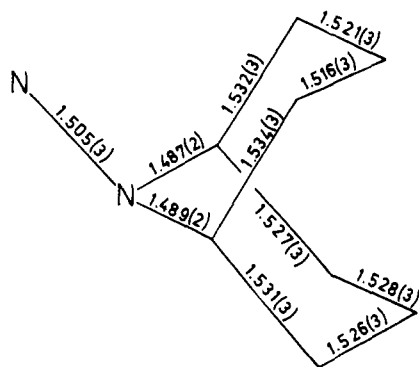


methyl compound **2** directly to the *N*-nitroso compound **5** (reaction g). Photolysis of tetrazene **7** gives **1** in 45% yield (after chromatography). Although abstraction of the hydrogens  $\alpha$  to nitrogen of the amino radical intermediate is not important because of Bredt's rule destabilization of the resulting imine, hydrogen atom abstraction (presumably from solvent) to give **4** is an important side reaction which decreases the yield of **1**. We found that the *N*-lithio compound couples with *N*-chloro compound **8** in good yield, but the fact that **4** is rather hygroscopic makes this reaction inconvenient. Treatment of the nonhygroscopic chloride **8** with 0.5 equiv of butyllithium in THF gives an excellent (92%) yield of **1**, and provides a convenient pathway from **2** to **1**. We presume that metal–halogen exchange gives the *N*-lithio compound, which undergoes electron transfer with **8**, because an  $\text{S}_{\text{N}}2$  reaction of these bulky compounds seems sterically unlikely.

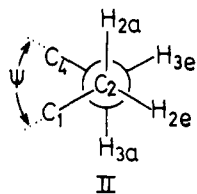
## Results and Discussion

Although the lone pair–lone pair dihedral angle  $\theta$  (see I) is gauche for 1,1'-bispiperidine and its five- to seven-membered

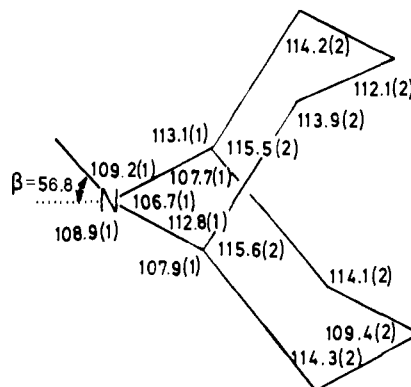
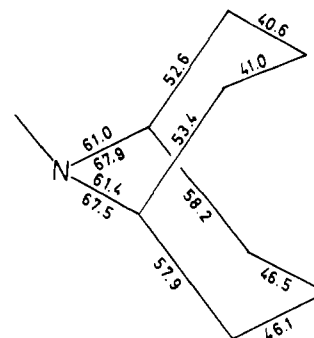


Figure 1. Thermal ellipsoid plot for **1** (30% probability ellipsoids).Figure 2. Bond lengths for **1**.

ring analogues,  $\theta$  is  $180^\circ$  for **1** (the midpoint of the N–N bond is a center of symmetry; see the thermal ellipsoid plot of Figure 1). This rotational angle is clearly forced by the bicyclic alkyl groups, as examination of molecular models will demonstrate. The bond lengths, bond angles, and dihedral angles for the heavy atoms are shown in Figures 2–4.<sup>11</sup> Both six-membered rings are in the expected chair forms, flattened as in other bicyclo[3.3.1]nonyl systems.<sup>12</sup> Such flattening decreases the  $H_{3a}$ – $H_{7a}$  nonbonded interaction (this distance was determined to be  $2.09_2$  Å for **1**). It is easiest to discuss this ring flattening in terms of the internal ring torsional angle  $\psi$  (the  $C_1C_2, C_3C_4$  dihedral angle, see II) and its counterparts ( $C_2C_3, C_4C_5; C_1C_8,$

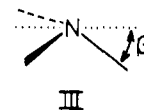


$C_7C_6$ ; and  $C_8C_7, C_6C_5$ ). The  $\psi$  (X-ray) angles are seen in Figure 4 to be  $40.8 \pm 0.2^\circ$  in the ring anti to the nitrogen lone pair and  $46.3 \pm 0.2^\circ$  in the ring syn to the lone pair. The average of these values is close to those calculated from the literature X-ray data for 1-brosylmethyl-5-methyl-9-hydroxybicyclo[3.3.1]nonane<sup>13</sup> ( $\psi$  values  $43.6$ – $45.2^\circ$ ) and 3-azabicyclo[3.3.1]nonane hydrobromide<sup>14</sup> ( $\psi$  averages  $43.0^\circ$  in the cyclohexane ring and  $50.2^\circ$  in the protonated piperidine ring). The solution NMR spectrum of **1** at 270 MHz was analyzed to give the coupling constants quoted in the experimental section. Using the  $R$  value technique,<sup>15</sup> in which  $R = (J_{aa} + J_{ee})/J_{ae} + J_{ea}$  for a  $-\text{CH}_2\text{CH}_2$  fragment of a six-membered ring, and the Buys relationship<sup>16</sup>  $\cos \psi = [3/(2 + 4R)]^{1/2}$ ,  $\psi$  (NMR) is calculated to be  $49.9^\circ$  ( $R = 1.31$ ), over  $6^\circ$  higher than the  $\psi$  (X-ray)<sub>av</sub> value of  $43.6^\circ$ . Because the Buys relationship assumes  $120^\circ$  projection angles for the  $\text{CH}_2$  frag-

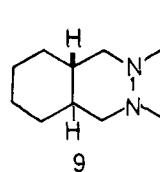
Figure 3. Bond angles for **1**.Figure 4. Torsional angles for **1**.

ments, it is perhaps not surprising that a larger discrepancy is observed for the very flattened rings of **1** than for several less distorted six-membered ring compounds, where  $\psi$  (NMR) only differs from  $\psi$  (X-ray) by  $1$ – $3^\circ$ .<sup>15</sup> We cannot rule out actual differences in solid and solution conformations as contributing to the discrepancy. The  $R$  values for three 1,5-diazabicyclo[3.3.1]nonane and -[3.2.1]octane derivatives which do not have an axial alkyl substituent on the one carbon bridge ranged from 1.17 to 1.26 ( $\psi$  (NMR)  $48$ – $49^\circ$ ),<sup>12</sup> close to that of **1**.

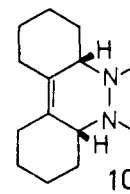
From the X-ray structures of **9** and **10** we argued<sup>4</sup> that both the pyramidal distortion angle  $\beta$ <sup>17</sup> (see III) and the N–N bond



length are sensitive to  $\theta$ , both increasing to minimize lone pair–lone pair interaction when  $\theta$  is near  $180^\circ$ . The  $\beta_{av}$  value<sup>17</sup> for **1** is only slightly smaller than those for **9**, and  $r(\text{N–N})$  is even longer. The increased bond length is not surprising, because the rings of **9** resist an N–N bond length increase, but



178–179°  
av 59.0, 59.6°  
 $r(\text{N–N})$  1.486(1) Å



70–74°  
av 47.3(eq), 51.0(ax)  
 $r(\text{N–N})$  1.450(3) Å

no such restoring force is present in **1**, and lengthening the N–N bond of **1** relieves  $H_1, H_1'$  nonbonded interaction, observed to be  $1.93_4$  Å, even smaller than the  $H_{3a}$ – $H_{7a}$  distance.

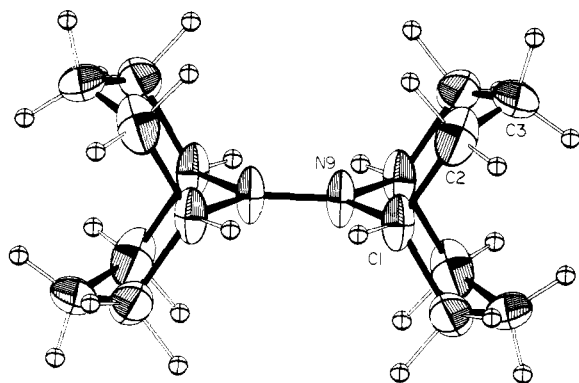


Figure 5. Thermal ellipsoid plot for  $1^+\cdot\text{PF}_6$  (30% probability ellipsoids).

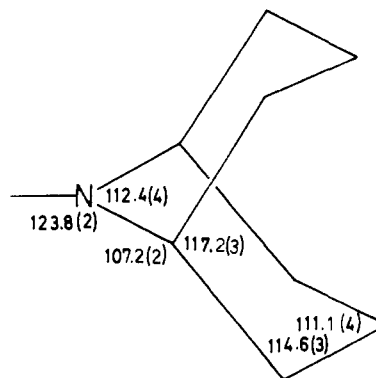


Figure 7. Bond angles for  $1^+$ .

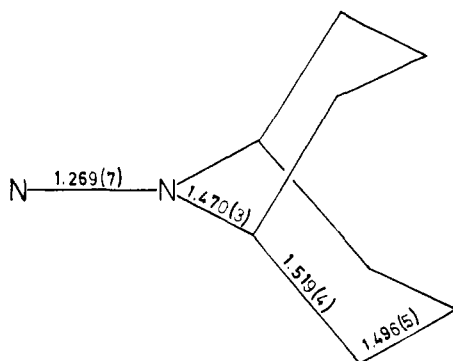


Figure 6. Bond lengths for  $1^+$ .

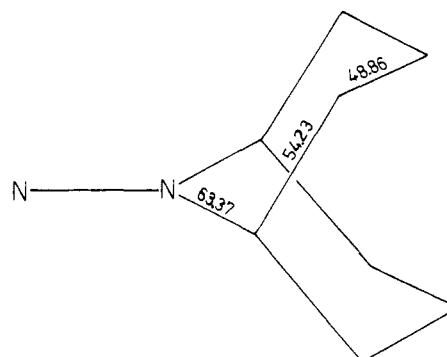


Figure 8. Torsional angles for  $1^+$ .

but quite comparable to the corresponding distance in adamantylideneadamantane, 1.90 Å.<sup>18</sup>

A thermal ellipsoid drawing of the  $1^+\cdot\text{PF}_6$  structure appears as Figure 5, and the bond distances, bond angles, and dihedral angles for the heavy atoms of  $1^+$  are shown in Figures 6–8.  $1^+$  lies on a special position of the crystal lattice, requiring that it possesses  $D_{2h}$  symmetry. There is a striking difference in the geometry at nitrogen in **1** and  $1^+$ . Electron removal completely flattens the nitrogens ( $\beta$  goes from 56.8 to 0.0°) and  $r(\text{NN})$  shortens by 0.237 Å (15.7%). A contention that the bicyclo[3.3.1]nonyl alkyl group structure of  $1^+$  enforces the flattening at nitrogen is not supportable. Not only are the nitrogens of neutral **1** bent past tetrahedral but  $\beta$  for the related nitroxide, 9-azabicyclo[3.3.1]nonan-3-one-9-oxyl,<sup>19</sup> is 30.5°, the largest yet determined for a nitroxide radical.<sup>20</sup> When the alkyl group structure sufficiently requires it, the equilibrium structure of a hydrazine radical cation can be nonplanar at nitrogen, as shown by ESR studies.<sup>6</sup>

The decrease in NN bond length upon electron removal from **1** is surprisingly large. Allmann<sup>21</sup> has discussed the relationship between bond order ( $n$ ) and bond length ( $r$ ) for C, N, and O terminus bonds in detail. The state of hybridization of these atoms is pointed out as significantly affecting bond length, and a table of  $r, n$  values for bonds between  $sp^2$ -hybridized atoms is given, using the Pauling formula<sup>22</sup>  $r(n) = r(1) - k \ln(n)$ ,  $k$  being derived in each case from literature data. Allmann points out that when  $sp^3$ -hybridized atoms are involved in the bond,  $r(1)$  is larger, and suggests addition of 0.03 Å for each  $sp^3$ -hybridized atom. The NN bond,  $r, n$  plot of Figure 9 shows Allmann's curve between  $n = 1$  and 2 as a solid line, and the crossed circle shows the value thus derived for a hydrazine bond length. The  $\theta$  sensitivity of  $r$  for hydrazines is illustrated with  $r(\text{NN})$  values for **1** and **9** ( $\theta$  180°), compared with those for H and alkyl-substituted gauche hydrazines;  $r(\text{NN})$  is experimentally 1.447–1.453 Å for  $\text{H}_2\text{NNH}_2$ , **10**, and 1,4-dimethylhexahydro-1,2,4,5-tetrazine.

Also shown are the  $r(\text{NN})$  values obtained for  $\text{H}_2\text{NNH}_3^+\text{CH}_3\text{CO}_2^-$  and  $\text{H}_3\text{NNH}_3^{2+}\text{SO}_4^{2-}$ .<sup>21</sup> The latter has a significantly shorter  $r(\text{NN})$ , conceivably because N lone pairs are absent, although the obvious charge difference must also affect the bond length observed. A range for nine azo compounds with saturated substituents<sup>21</sup> is included at  $n = 2$ , and a linear extrapolation for Allmann's curve to  $n = 3$  (the  $\text{N}_2$  molecule) is shown as a dotted line. It is interesting that  $r(\text{N}\equiv\text{N})$  values for three aryldiazonium salts are in the range 1.10–1.11 Å.<sup>23</sup> Any charge-induced shortening is more than balanced by conjugative lengthening in these systems.

We point out that  $1^+$ , which has  $sp^2$ -hybridized nitrogens and three  $\pi$  electrons, one of which must be antibonding so the formal bond order is 1.5, has an anomalously short bond length ( $n$  is about 1.77, using the Allmann curve). It is useful to compare the bond length for  $1^+$  with those of the isoelectronic (and uncharged) nitroxide radicals, which have been extensively studied,<sup>20</sup> to see if a similar anomalous shortening of the NO bond is observed. An  $r, n$  plot for NO bonds appears as Figure 10. The Allmann curve between  $n = 1$  and 2 (solid line a) is seen to be in serious error, especially when extrapolation to  $n = 3$  ( $\text{NO}^+$ ) is considered. The problem is in defining  $r(n = 2)$ . Linnett and Rosenberg<sup>24</sup> have argued that, although HNO does have  $n = 2$ , XNO molecules with X = F, Cl, and Br have  $n = 2.5$ ; the latter were apparently used with  $n = 2$  to define curve a. When  $k$  is estimated using the 1.212 N=O bond length of HNO, solid line b is obtained. Using curve b, the NN and NO  $r, n$  plots are quite similar, as expected from the numerical identity of the covalent bond radii for N and O.<sup>22</sup> Accurate structural data have been determined for ten dialkyl nitroxides, the total range of  $r(\text{NO})$  values being indicated in Figure 10. For six piperidine-*N*-oxyl derivatives,  $r$  averages 1.284 (range 1.296–1.274), and  $\beta$  is 15.8–30.5° (except for one example, where  $\beta$  is 0°), marginally longer than for four pyrrolidine-*N*-oxyl derivatives, for which  $r$  averages 1.273 (range 1.266–1.283) and  $\beta$  is 0° (3.3° for one example). The differ-

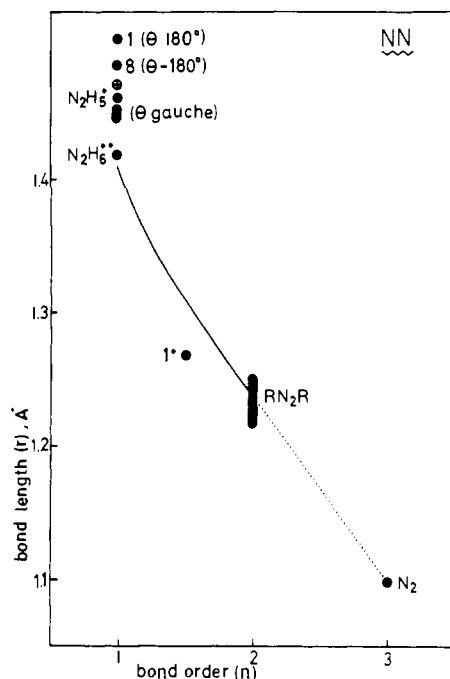


Figure 9. Bond length, bond order ( $r,n$ ) plot for NN bonded systems.

ences in  $r(\text{NO})$  found could reflect the expected lengthening of the NO bond as the nitrogen becomes nonplanar. The deviation observed for nitroxide NO bond lengths from the  $r,n$  curve is substantially less than that observed for  $1^+$ . It is clear that steric effects will tend to lengthen the NN bond of  $1^+$ , not shorten it. We suggest that the most likely reason for the shorter NN bond of  $1^+$  than that expected is a charge effect. We note that  $\text{NO}^+$  has a 0.036 Å shorter bond than  $\text{N}_2$ , even though compression is more difficult when  $r$  is short than when it is longer. The deviation to shorter bond length observed for  $1^+$  seems to be of a reasonable magnitude, considering this. This work shows that use of the Pauling equation to predict the NN bond length for a hydrazine radical cation leads to considerable error. The description of  $1^+$  as possessing an “olefin-like” structure is a good one.

### Experimental Section

**9-Methyl-9-azabicyclo[3.3.1]nonane (2)**<sup>25</sup> was prepared by Wolff-Kishner reduction of pseudopellitterine,<sup>26</sup> a reaction reported<sup>27</sup> without experimental details. KOH (85%, 60.34 g, 0.914 mol) pellets were dissolved in 750 mL of diethylene glycol in a 2-L flask equipped with a reflux condenser and distillation head, and after cooling to 50 °C, 42.12 g (0.842 mol) of hydrazine hydrate and 36.13 g (0.236 mol) of pseudopellitterine were added. After heating for 2 h until most of the excess water and hydrazine were distilled off, the mixture was heated in a Wood's metal bath (ca. 230 °C) for 3 h, cooled to room temperature, combined with the distillate, and diluted with 750 mL of water. Extraction with 3 × 250 mL of ether, washing with 100 mL of  $\text{H}_2\text{O}$ , drying over  $\text{MgSO}_4$ , filtration, and concentration gave an oil which was sublimed to give 28.09 g (85.6%) of **2**, mp 53–57 °C (lit.<sup>27</sup> mp 55–58 °C).

**9-Nitroso-9-azabicyclo[3.3.1]nonane (5)**. The general nitrosative cleavage of Smith and Loepky<sup>28a</sup> was employed. A solution of 29.3 g (0.42 mol) of  $\text{NaNO}_2$  in 50 mL of water was added over 30 min to a mixture of 5.12 g (36.8 mmol) of amine **2**, 100 mL of acetic acid, 200 mL of water, and 25.25 g of sodium acetate. The greenish-yellow solution was gently heated on a steam bath without stirring to an internal temperature of about 60 °C for 7 days. Extraction with 3 × 100 mL of ether, careful wash with sodium carbonate solution until the aqueous layer remained strongly basic, drying, and concentration gave 3.38 g (21.9 mmol, 60%) of **5**, mp 149–151 °C (lit.<sup>28b</sup> 148 °C). Starting material was recovered by basicifying the aqueous layer and extracting with ether; the conversion is over 90%. For **5**:  $^1\text{H}$  NMR ( $\text{CDCl}_3$ ,  $\text{Me}_4\text{Si}$ )  $\delta$  5.28 (m, 1 H), 4.88 (m, 1 H), 2.5–1.4 (m, 12 H);

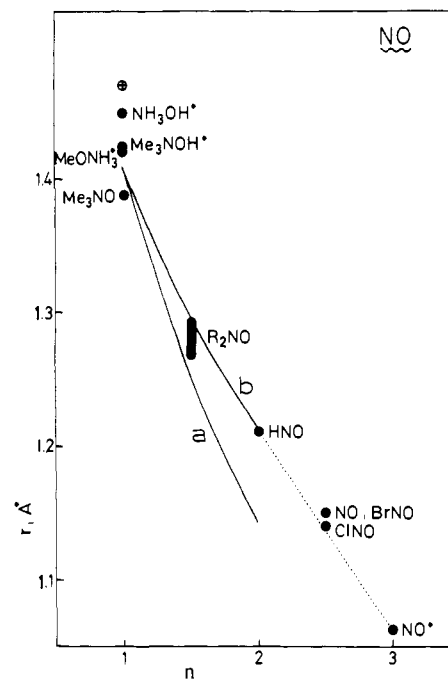


Figure 10. Bond length, bond order ( $r,n$ ) plot for NO bonded systems. Curve a is taken from Allmann's table,<sup>21</sup> and b uses HNO to establish the  $r(\text{N}=\text{O})$  bond length (see text).

$^{13}\text{C}$  NMR ( $\text{CDCl}_3$ ,  $\text{Me}_4\text{Si}$ )  $\delta$  54.4, 43.4, 31.4, 29.3, 20.1; IR ( $\text{CCl}_4$ ) no absorption 2800–1500  $\text{cm}^{-1}$ .

**Phenyl-9-carboxy-9-azabicyclo[3.3.1]nonane (3)**.<sup>25</sup> After the general method of Hobson and McClusky,<sup>29</sup> 27.57 g (0.198 mol) of **2** and 100 mL of dichloromethane (distilled from calcium hydride) were stirred at 0–5 °C while a solution of 31.04 g (0.198 mol) of freshly distilled phenyl chloroformate in 50 mL of dichloromethane was added over 5 min. After 10 min of stirring, the mixture was allowed to warm to room temperature as it stirred for 4 h. The mixture was washed with 130 mL of 15% aqueous NaOH, 150 mL of 1 M HCl, and 100 mL of  $\text{H}_2\text{O}$ , and each aqueous wash was back-extracted with 50 mL of dichloromethane. Drying and concentration gave a solid (44.9 g), which was crystallized from hexane to give 35.5 g (0.145 mol, 73%) of **3**, mp 100–102.5 °C. Although more **3** was present in the mother liquor, it was considerably less pure. For **3**:  $^1\text{H}$  NMR ( $\text{CDCl}_3$ )  $\delta$  7.0–7.6 (m, 5 H), 4.2–4.7 (m, 2 H), 1.2–1.4 (m, 12 H); IR ( $\text{CCl}_4$ ) 1715  $\text{cm}^{-1}$ .<sup>30</sup>

**9-Azabicyclo[3.3.1]nonane (4)**.<sup>31</sup> A mixture of 15.07 g (61.5 mmol) of **3**, 200 mL of 95% ethanol, 70 mL of water, 24.4 g (0.61 mol) of sodium hydroxide pellets, and 0.76 g of tetrabutylammonium iodide was refluxed for 42 h. After cooling and addition of concentrated HCl until the mixture was strongly acidic, it was heated at reflux until  $\text{CO}_2$  evolution ceased (1 h). After removal of ethanol, the mixture was diluted with water to 500 mL and extracted with two 150-mL portions of ether. After cooling and basicification with KOH pellets, the amine was extracted with 4 × 150 mL of ether. After drying, filtration, and concentration, 4.48 g (35.8 mmol, 58%) of **4** was obtained as a hygroscopic, very volatile solid which was usually stored as the hydrochloride, mp 345–350 °C. For **4**: NMR ( $\text{CDCl}_3$ )  $\delta$  3.7 (br s, integrating for 2 H—sample undoubtedly wet), 3.0–3.4 (m, 2 H), 1.5–2.3 (m, 12 H).

**9-Amino-9-azabicyclo[3.3.1]nonane (6)**<sup>32</sup> was prepared by addition of 4.53 g (29.4 mmol) of **5** in 100 mL of ether to a suspension of 3.44 g (90.7 mmol) of lithium aluminum hydride in 50 mL of ether, followed by 1.5 h of reflux and stirring at room temperature for 65 h, followed by the workup of Micovic and Mihailovic.<sup>33</sup> After drying and concentration, the residue was crystallized from ether/hexane at –78 °C, giving 2.89 g (20.6 mmol, 70%) of **6**, mp 97–119 °C (the monohydrate has mp 50–52 °C<sup>33</sup>). NMR ( $\text{CDCl}_3$ )  $\delta$  1.3–2.3 (m, 12 H), 2.8–3.03 (m, 2 H), 3.47 (br s, 2 H); IR ( $\text{CCl}_4$ ) 3500–3100 (br), 3240  $\text{cm}^{-1}$ , no C=O stretch observed.<sup>30</sup>

**Azo-9-azabicyclo[3.3.1]nonane (7)**. A solution of 1.37 g (9.79 mmol) and 4 mL of diethylamine in 100 mL of  $\text{Et}_2\text{O}$  was cooled in an ice bath under nitrogen while a solution of 2.5 g of iodine in 80 mL of ether was

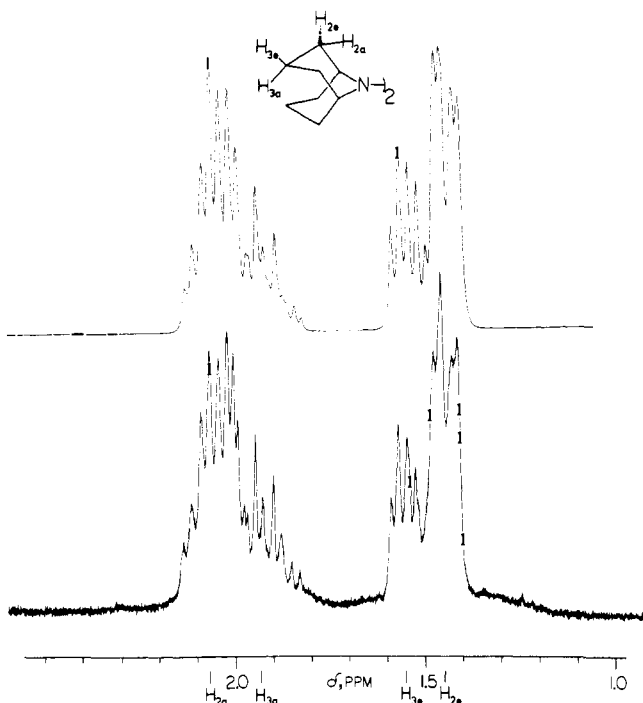


Figure 11.  $H_{2a}$ ,  $H_{2e}$ ,  $H_{3a}$ ,  $H_{3e}$  region of the NMR of **1** calculated with the parameters of Table I, compared with the experimental spectrum.

dripped in until a yellow color persisted (over 2 h, about three-quarters of the iodine solution had been added). The reaction mixture was filtered, washed with 75 mL of 10% sodium thiosulfate and 75 mL of water, and dried (magnesium sulfate). Concentration gave a residue (1.26 g) which was recrystallized from pentane to give 0.69 g (2.5 mmol, 51%) of **7**: mp 156–158 °C dec (gas evolution);  $^1\text{H}$  NMR ( $\text{CDCl}_3$ ,  $\text{Me}_4\text{Si}$ )  $\delta$  4.06 (br s, 4 H), 1.2–2.4 (m, 24 H);  $^{13}\text{C}$  NMR ( $\text{CDCl}_3$ ,  $\text{Me}_4\text{Si}$ )  $\delta$  50.51, 28.32, 20.87; IR no NH stretch.<sup>30</sup>

**9-Chloro-9-azabicyclo[3.3.1]nonane (8)**. Solid 9-azabicyclo[3.3.1]nonane hydrochloride (2.0 g, 12.4 mmol) was added to a vigorously stirred solution of 25 mL of Clorox (0.628 M NaOCl, 16 mmol) in 25 mL of ether cooled to 0 °C, the ice bath removed, and the solution stirred for 15 min as the mixture warmed to room temperature. The bottom layer was removed by a pipet and 25 mL of fresh Clorox added. After an additional 15 min of vigorous stirring, the layers were separated and the combined aqueous layers extracted with ether. After drying, filtration, and concentration, the residue was sublimed to give a glassy solid, 1.45 g (9.1 mmol, 73%): mp 71.5–73 °C; NMR ( $\text{CDCl}_3$ ,  $\text{Me}_4\text{Si}$ )  $\delta$  3.28 (br s, 2 H), 1.2–2.8 (m, 12 H); IR no NH stretch.<sup>30</sup>

**9,9-Bis-9-azabicyclo[3.3.1]nonane (1)**. **A. By Photolysis of Tetrazene 7**. A deaerated solution of 0.5 g (1.81 mmol) of the tetrazene in 200 mL of cyclohexane was irradiated for 45 min with a 450-W medium-pressure Hanovia lamp in a Pyrex immersion well. After concentration the residue was chromatographed with a 2:1 mixture of ethyl acetate–benzene on a silica gel PF-254 plate, giving 0.20 g (0.81 mmol, 45%) of **1** as the first band ( $R_f$  0.5). Sublimation gave 0.14 g (31%) of pure **1**: mp 140–142 °C;  $^1\text{H}$  NMR ( $\text{CDCl}_3$ ,  $\text{Me}_4\text{Si}$ )  $\delta$  3.22 (br s, 4 H), 1.2–2.3 (m, 24 H);  $^{13}\text{C}$  NMR ( $\text{CDCl}_3$ ,  $\text{Me}_4\text{Si}$ )  $\delta$  47.04, 27.71, 20.87; IR ( $\text{CCl}_4$ ) no NH stretch.<sup>30</sup>

**B. By Coupling of 8**. Butyllithium (0.99 mL, 1.52 mmol of 1.55 M hexane solution) was added to 0.49 g (3.07 mmol) of **8** in 10 mL of dry THF at –78 °C. After stirring for 30 min, the mixture was allowed to warm to room temperature as it stirred for 1 h, extracted with 10% sodium carbonate solution, dried, filtered, and concentrated, to give 0.35 g (1.41 mmol, 92%) of **1**.

**9,9'-Bis-9-azabicyclo[3.3.1]nonenium Hexafluorophosphate (1<sup>+</sup>PF<sub>6</sub>)**. Addition of 58.7 mg (0.336 mmol) of nitrosyl hexafluorophosphate to a solution of 83.4 mg (0.336 mmol) of **1** in 3 mL of acetonitrile and 5 mL of methylene chloride gave immediate yellow coloration and gas evolution. After stirring for 30 min, concentration yielded 129.8 mg (0.300 mmol, 98%) of yellow 1<sup>+</sup>PF<sub>6</sub>, which was recrystallized in low yield from either methylene chloride/chloroform mixtures or ethanol to give clear yellow plates, mp 283–286 °C dec. Anal. Calcd

Table I.  $^1\text{H}$  NMR Data for **1**

hydrogen	$\delta$ , ppm	coupling constants
$H_1$	3.18	$J(H_1-H_{2a}) = 5.2_9$
$H_{2a}$	2.06	$J(H_1-H_{2e}) = -0.5_8$
$H_{2e}$	1.45	$J(H_{2a}-H_{2e}) = 12.8_5$
$H_{3a}$	1.93	$J(H_{2a}-H_{3e}) = 5.9_6$
$H_{3e}$	1.55	$J(H_{2a}-H_{3a}) = 13.7_1$
		$J(H_{2e}-H_{3e}) = +0.4_9$
		$J(H_{2e}-H_{3a}) = 4.8_9$
		$J(H_{3e}-H_{3a}) = 12.7_6$

Table II. Fractional Coordinates ( $\times 10^4$ ) and Isotropic Temperature Factors for **1**<sup>a</sup>

atom	x	y	z	$B_{\text{iso}}$
C1	2997 (3)	5632 (3)	3240 (2)	
C2	323 (3)	4572 (3)	2415 (2)	
C3	-819 (3)	2036 (3)	1749 (2)	
C4	305 (3)	870 (3)	2977 (2)	
C5	2976 (3)	2060 (3)	3771 (2)	
C6	4164 (4)	1953 (3)	2711 (2)	
C7	3930 (4)	3447 (3)	1483 (2)	
C8	4208 (4)	5753 (3)	2156 (2)	
N9	3694 (2)	4424 (2)	4537 (1)	
H1	3460 (29)	7160 (31)	3744 (20)	2.7 (3)
H2A	-230 (35)	4834 (34)	3201 (25)	4.4 (5)
H2B	-148 (35)	5444 (34)	1602 (25)	4.5 (4)
H3A	-724 (32)	1645 (32)	753 (24)	3.9 (4)
H3B	-2425 (36)	1450 (31)	1498 (23)	3.9 (4)
H4A	-209 (36)	-721 (39)	2537 (25)	4.9 (5)
H4B	-230 (36)	810 (35)	3854 (27)	5.1 (4)
H5	3414 (27)	1257 (26)	4587 (19)	2.2 (3)
H6A	5805 (35)	2430 (31)	3401 (22)	3.6 (4)
H6B	3555 (34)	360 (38)	2217 (23)	4.2 (4)
H7A	2438 (34)	2672 (31)	575 (23)	3.5 (4)
H7B	5103 (36)	3701 (35)	1074 (24)	4.6 (5)
H8A	3575 (30)	6454 (30)	1295 (23)	3.5 (4)
H8B	5834 (35)	6700 (33)	2772 (22)	3.7 (4)

<sup>a</sup> Standard deviations of the last significant figure are given in parentheses in this and in all following tables.

for  $\text{C}_{16}\text{H}_{28}\text{N}_2\text{PF}_6$ : C, 48.85; H, 7.17; N, 7.12. Found: C, 48.79; H, 7.01; N, 7.18.

**Simulation of  $^1\text{H}$  NMR of **1****. The 270-MHz NMR of **1** in  $\text{CDCl}_3$ - $\text{Me}_4\text{Si}$  solution (Bruker WH 270 spectrometer) was simulated using the literature program NUMARIT<sup>34</sup> on a Harris Slash 7 computer interfaced with a Calcomp 836 plotter. Since NUMARIT is limited to seven spin systems and one plane of symmetry, the following simplification was made. The spectrum was simulated by neglecting all protons on one side of the plane defined by the bridgehead protons and the nitrogen atom. Although this reduces by one-half the number of protons coupling with  $H_1$  ( $\delta$  3.2), there should be no effect on the spectrum in the region of interest, 1.0–2.5 ppm, where  $H_{2a}$ ,  $H_{2e}$ ,  $H_{3a}$ , and  $H_{3e}$  appear. Iteration was performed by matching 23 observed transitions with calculated ones in the 1–2.5-ppm region, and matching an observed transition with a calculated one so that the calculated shift equals the observed one for  $H_1$  at  $\delta$  3.18. Input parameters were obtained by decoupling experiments, and NUMARIT converged to a root mean square deviation of 0.39 Hz, giving the values quoted in Table I. A plot of experimental and calculated spectra appears as Figure 11.

**Crystallography for **1****.  $\text{C}_{16}\text{H}_{28}\text{N}_2$ ; mol wt 176.35; colorless prism.  $0.30 \times 0.18 \times 0.25$  mm by evaporation from  $\text{CH}_2\text{Cl}_2$ ; triclinic,  $a = 6.887$  (2) Å,  $b = 6.514$  (2) Å,  $c = 9.380$  (2) Å,  $\alpha = 91.45$  (2)°,  $\beta = 112.74$  (2)°,  $\gamma = 112.82$  (2)°,  $V = 350.0$  (2) Å<sup>3</sup>;  $Z = 1$ ; space group,  $P\bar{1}$ ;  $d_c = 1.178$  g/cm<sup>3</sup>;  $d_m = 1.17$  g/cm<sup>3</sup>;  $\mu = 0.460$  cm<sup>-1</sup>; Syntex PT diffractometer; Mo  $K\alpha$  graphite monochromated radiation; data at 2–24°/min via  $\theta$ - $2\theta$  scans, fixed background;  $3^\circ \leq 2\theta \leq 50^\circ$ ; standard reflections 2/50 <2% variation; 1144 unique data; 892 data with  $I \geq 2(I)$ ;  $p = 0.055$ ;<sup>35</sup> solution by direct methods;<sup>36</sup>  $R_1 = 8.1\%$ ,  $R_2 = 10.2\%$ <sup>37</sup> at isotropic convergence;<sup>38</sup>  $R_1 = 4.0\%$ ,  $R_2 = 4.8\%$  at anisotropic convergence (hydrogens isotropic); esd of an observation at unit

**Table III.** Fractional Coordinates ( $\times 10^4$ ) and Isotropic Temperature Factors for  $1^+\cdot\text{PF}_6^-$ 

atom	x	y	z	$B_{\text{iso}}$
Pl	0	0	0	
F1	2133 (3)	-24 (3)	0	
F2	0	0	930 (3)	
N9	5000	5000	381 (2)	
C1	3834 (3)	3834	874 (2)	
C2	5060 (6)	2584 (4)	1349 (2)	
C3	6475 (5)	3525	1836 (3)	
H1	3154 (43)	3154	539 (27)	8.1 (12)
H2A	5666 (53)	1620 (55)	936 (23)	9.4 (10)
H2B	4083 (46)	1978 (52)	1695 (23)	8.0 (9)
H3A	5953 (68)	4047	2309 (39)	10.0 (17)
H3B	7343 (55)	2657	1976 (29)	9.4 (15)
$F^*a$	1576 (61)	114 (51)	-543 (22)	3.1 (6)

<sup>a</sup> Disordered fluorine atom; the multiplicities of atoms F1, F2, and  $F^*$  were 0.479, 0.240, and 0.031, respectively; see text.

weight, 1.15; data/parameters 6.46 (892/138); maximum residual difference electron density, 0.1 e.

This structure was solved and refined by routine crystallographic procedures. Bond lengths and angles with estimated standard deviations from the full inversion matrix are shown in Figures 2 and 3. Final atom coordinates are listed in Table II. Anisotropic thermal parameters and structure factor amplitudes are listed in the supplementary material.

**Crystallography for  $1^+\cdot\text{PF}_6^-$ .**  $\text{C}_{16}\text{H}_{28}\text{N}_2\text{PF}_6$ ; mol wt 393.39; yellow hexagonal prism  $0.17 \times 0.20 \times 0.35$  mm from vapor diffusion of pentane into  $\text{CH}_2\text{Cl}_2$  solution at  $0^\circ\text{C}$ ; tetragonal,  $D_{4h}$ ; cell parameters ( $20^\circ\text{C}$ )  $a = b = 7.468$  (2)  $\text{\AA}$ ,  $c = 16.635$  (5)  $\text{\AA}$ ,  $V = 927.7$  (4)  $\text{\AA}^3$ ; cell parameters ( $-60^\circ\text{C}$ )  $a = b = 7.407$  (2)  $\text{\AA}$ ,  $c = 16.629$  (10)  $\text{\AA}$ ,  $V = 912.4$  (7)  $\text{\AA}^3$ ;  $Z = 2$ ;  $d_c = 1.407$   $\text{g/cm}^3$ ;  $d_m = 1.403$   $\text{g/cm}^3$ ;  $\mu = 2.004$   $\text{cm}^{-1}$ ; systematic absences  $h0l$ ,  $h + l = 2n = 1$ ; space group  $P4_2/mnm$  ( $D_{4h}^2$ , no. 136); Syntex PT diffractometer; Mo  $K\alpha$  graphite monochromated radiation; data ( $-60^\circ\text{C}$ ) at  $2-24^\circ/\text{min}$  via  $\theta-2\theta$  scans, fixed background  $5^\circ < 2\theta < 60^\circ$ ; standards 2/50, < 1% variation; 759 unique data; 525 with  $I \geq 2\sigma(I)$  excluding (002), (013), (100) due to counter saturation;  $p = 0.055$ . Solved by heavy atom method:  $R_1 = 6.3\%$ ,  $R_2 = 8.2\%$  at anisotropic convergence (hydrogens isotropic); esd of an observation at unit weight, 2.08; data/parameters, 8.7 (524/60); maximum residual difference electron density, 0.3 e.

The solution and refinement of this crystal structure were complicated by the choice of three possible space groups ( $P4_2/mnm$ ,  $P4n2$  ( $D_{2d}^8$ , no. 118),  $P4_2nm$  ( $C_{4v}^2$ , no. 102)), and by the occurrence of what was eventually determined to be a slight disorder of the  $\text{PF}_6^-$  anions. The initial room temperature data (342 reflections) were solved and refined using the centric space group  $P4_2/mnm$ , which requires each atom except C(2) to be constrained to a different special position, thus further reinforcing the space group choice. However, the unsatisfactory  $R_1$ ,  $R_2$ , and goodness of fit parameters of 8.5, 9.8, and 2.18, respectively, and the relatively large thermal parameters on the  $\text{PF}_6^-$  fluorine atoms led us to recollect the data with a larger crystal, at a lower temperature, in order to improve the data to parameter ratio to allow refinement in the two acentric space group choices. For this data set (524 reflections) the centric refinement converged isotropically to  $R_1 = 26.4\%$  and  $R_2 = 36.4\%$ . Inclusion of hydrogen atoms and allowing anisotropic thermal motion for the nonhydrogen atoms caused  $R_1$  and  $R_2$  to drop to 7.0 and 9.0%, respectively. Attempted refinement in either acentric space group resulted in meaningless distortions of chemically equivalent bond lengths while not significantly improving agreement between  $F_{\text{obsd}}$  and  $F_{\text{calcd}}$ . It is interesting to note that in all three refinements the N-N bond length did not change by more than  $2\sigma$ . On close examination of the centric electron density difference map, many weak peaks of 0.3 e or less were observed in the vicinity of the  $\text{PF}_6^-$  anion. When the largest of these was included in the least-squares refinement, its multiplicity factor refined to a value corresponding to a 4.1% disorder of the  $\text{PF}_6^-$  anion and  $R_1$  and  $R_2$  converged to 6.3 and 8.2%. In the final difference map the largest peak, 0.3 e, was located near the symmetry position between the nitrogens, while the remaining peaks were within 0.9  $\text{\AA}$  of the  $\text{PF}_6^-$  atoms. Final atomic coordinates are listed in Table III. Anisotropic thermal parameters and structure factor amplitudes are included in the supple-

mentary material. Bond lengths and angles with standard deviations estimated from the full inversion matrix are presented in Figures 6 and 7.

**Acknowledgments.** We thank the National Science Foundation for partial financial support of this work both through the Major Instrument Program and Grant MPS 74-19688.

**Supplementary Material Available:** Tables of anisotropic temperature factors for the heavy atoms, and observed and calculated structure factors for **1** and  $1^+\cdot\text{PF}_6^-$  (9 pages). Ordering information is given on any current masthead page.

## References and Notes

- (1) For a review of hydrazine conformational work see Shvo, Y. In "The Chemistry of Hydrazo, Azo, and Azoxy Groups", Part 2: S. Patai, Ed.; Wiley: New York, N.Y., 1975; pp 1017-1095.
- (2) (a) Rademacher, P. *Angew. Chem.* **1973**, *85*, 410. (b) *Tetrahedron Lett.* **1974**, *83*, *Chem. Ber.* **1975**, *108*, 1548. Rademacher, P.; Koopman, W. *ibid.* **1975**, *108*, 1557.
- (3) (a) Nelsen, S. F.; Buschek, J. M. *J. Am. Chem. Soc.* **1973**, *95*, 2011. (b) Nelsen, S. F.; Buschek, J. M.; Hintz, P. J. *ibid.* **1973**, *95*, 2013. (c) Nelsen, S. F.; Buschek, J. M. *ibid.* **1974**, *96*, 2392. (d) *ibid.* **1974**, *96*, 6982. (e) *ibid.* **1974**, *96*, 6987.
- (4) Nelsen, S. F.; Hollinsed, W. C.; Calabrese, J. C. *J. Am. Chem. Soc.* **1977**, *99*, 4461.
- (5) (a) Adams, J. Q.; Thomas, J. R. *J. Chem. Phys.* **1963**, *39*, 1904. (b) Marquardt, C. L. *ibid.* **1970**, *53*, 3248. (c) Reilly, M. N.; Marquardt, C. L. *ibid.* **1970**, *53*, 3257. (d) Brivati, J. A.; Gross, J. M.; Symons, M. C. R.; Timling, J. A. *J. Chem. Soc.* **1965**, 6504. (e) Fantechi, R.; Helcke, G. A. *J. Chem. Soc., Faraday Trans. 2* **1972**, *68*, 924.
- (6) (a) Nelsen, S. F.; Weisman, G. R.; Hintz, P. J.; Olp, D.; Fahey, M. R. *J. Am. Chem. Soc.* **1974**, *96*, 2916. (b) Nelsen, S. F.; Echegoyen, L. *ibid.* **1975**, *97*, 4930.
- (7) Nelsen, S. F.; Peacock, V.; Weisman, G. R. *J. Am. Chem. Soc.* **1976**, *98*, 5269.
- (8) Nelsen, S. F.; Hintz, P. J.; Buschek, J. M.; Weisman, G. R. *J. Am. Chem. Soc.* **1976**, *98*, 3281.
- (9) Nelsen, S. F.; Kessel, C. R. *J. Am. Chem. Soc.* **1977**, *99*, 2392.
- (10) Nelsen, S. F.; Kessel, C. R. *J. Chem. Soc., Chem. Commun.* **1977**, 490.
- (11) Anisotropic temperature factors for the heavy atoms and observed and calculated structure factors appear in the supplementary material (see paragraph at end of paper).
- (12) Nelsen, S. F.; Hintz, P. J.; Landis, R. T., II. *J. Am. Chem. Soc.* **1972**, *94*, 7105.
- (13) Brown, W. A. C.; Martin, J.; Sim, G. A. *J. Chem. Soc.* **1965**, 1844.
- (14) Döbler, M.; and Dunitz, J. D. *Helv. Chim. Acta* **1964**, *47*, 695.
- (15) Lambert, J. B. *Acc. Chem. Res.* **1971**, *4*, 87.
- (16) Buys, H. R. *Recl. Trav. Chim. Pays-Bas* **1969**, *88*, 1003.
- (17)  $\beta_{\text{av}}$  is the average of the three  $\beta$  values for an asymmetric nitrogen.  $\beta_{\text{av}}$  is very closely approximated ( $< 0.4^\circ$  error even when the  $\alpha$  values cover a  $9^\circ$  range) by  $\beta_{\text{av}} = \arccos(\cos(180^\circ - \alpha_{\text{av}})/\cos(\alpha_{\text{av}}/2))$ , where  $\alpha_{\text{av}} = (\alpha_1 + \alpha_2 + \alpha_3)/3$  (see i). When  $\alpha_2 = \alpha_3$   $\beta = \arccos(\cos(180 - \alpha_2)/\cos(\alpha_1/2))$  is exact.  $\beta$  is seen to be more sensitive to small deviations from planarity than is  $\alpha - \beta$  is  $24.3^\circ$  when  $\alpha = 118^\circ$  and  $34.2^\circ$  when  $\alpha = 116^\circ$ .
- (18) Lidd, R. D.; Mann, D. E. *J. Chem. Phys.* **1958**, *28*, 572.
- (19) Capiomont, A.; Chion, B.; Lajzerowicz, J. *Acta Crystallogr., Sect. B* **1971**, *27*, 322.
- (20) Lajzerowicz-Bonneteau, J. "Spin Labeling", Berliner, L. J., Ed; Academic Press: New York, N.Y., 1976; pp 239-249.
- (21) Allmann, R. In ref 1, Part 1, pp 23-52.
- (22) Pauling, L. "The Nature of the Chemical Bond", Cornell University Press: Ithaca, N.Y., 1960.
- (23) Wyckoff, R. W. G. "Crystal Structures", Vol. 6; Part 1; 2nd ed.; Wiley-Interscience: New York, N.Y., 1966; entries all,32, all,33, and all,37.
- (24) Linnett, J. W.; Rosenberg, R. M. *Tetrahedron* **1964**, *20*, 53.
- (25) Weisman, G. R. Ph.D. Thesis, University of Wisconsin, **1976**.
- (26) Cope, A. C.; Dryden, H. L., Jr.; Howell, C. F. "Organic Syntheses", Collect. Vol. IV; Wiley: New York, N.Y., 1963; p 816.
- (27) Fisch, M. H.; Gramain, J. C.; Olesen, J. A. *J. Chem. Soc., Chem. Commun.* **1971**, 663.
- (28) (a) Smith, P. A. S.; Loeppky, R. N. *J. Am. Chem. Soc.* **1967**, *89*, 1147. (b) Ciamician, G.; Silber, P. *Chem. Ber.* **1894**, *27*, 2850.
- (29) Hobson, J. D.; McClusky, J. G. *J. Chem. Soc. C* **1967**, 2015.
- (30) Empirical formula established by high-resolution mass spectroscopy.
- (31) Stetter, H.; Heckel, K. *Chem. Ber.* **1975**, *106*, 339.
- (32) Jucker, E.; Lindenman, A. *J. Chem. Abstr.* **1966**, *64*, 3496a.
- (33) Mićović, V. M.; Mihailović, M. L. *J. Org. Chem.* **1953**, *18*, 1190.
- (34) (a) NUMARIT is a modification of NUMAR<sup>3d</sup> by K. M. Worvill (University of East Anglia) and J. S. Martin (University of Alberta). We thank P. M. Treichel and D. R. Berg (University of Wisconsin) for making it available to us. (b) Quirt, A. R. Ph.D. Thesis, University of Alberta, 1972.
- (35) For crystallographic details see Teo, B. K.; Calabrese, J. C. *Inorg. Chem.* **1976**, *15*, 2474.



(36) Programs used in the solution and refinement of the structures included MULTAN (Germain, Main, Woolfson), ORFLS and ORFFE (Busing, Martin, Levy), and ORTEP (C. K. Johnson). Remaining programs were written by J. C. Calabrese.

(37)  $R_1 = \frac{\sum |F_o| - |F_c|}{\sum |F_o|}$  and  $R_2 = \frac{\sum w_i |F_o| - |F_c|}{\sum w_i |F_o|^2}$

(38) All least-squares refinements were based on the minimization of  $\sum w_i |F_o| - |F_c|$  with the individual weights  $w_i = 1/\sigma(F_o)^2$ . Atomic scattering factors used for all nonhydrogen atoms are from Hanson, H. P.; Herman, F.; Lea, J. D.; Skillman, S. *Acta Crystallogr.* **1964**, *17*, 1040. Those for the hydrogen atoms are from Stewart, R. F.; Davidson, E. R.; Simpson, W. T. *J. Chem. Phys.* **1965**, *42*, 3175.

## Specific Sequestering Agents for the Actinides. 2. A Ligand Field Effect in the Crystal and Molecular Structures of Tetrakis(catecholato)uranate(IV) and -thorate(IV)<sup>1</sup>

Stephen R. Sofen, Kamal Abu-Dari, Derek P. Freyberg, and Kenneth N. Raymond\*

Contribution from the Department of Chemistry and Materials and Molecular Research Division, Lawrence Berkeley Laboratory, University of California, Berkeley, California 94720. Received May 10, 1978

**Abstract:** The structures of the title compounds,  $\text{Na}_4[\text{M}(\text{C}_6\text{H}_4\text{O}_2)_4] \cdot 21\text{H}_2\text{O}$ ,  $\text{M} = \text{Th}, \text{U}$ , have been determined by single-crystal X-ray diffraction methods using counter data. These isostructural tetrakis(catecholato) complexes are structural archetypes for actinide-specific macrocyclic sequestering agents. The complexes have  $D_{2d}$  molecular symmetry. The M–O bond lengths are 2.417 (3) and 2.421 (3) Å for Th and 2.362 (3) and 2.389 (4) Å for U. The ring O–M–O bond angles are 66.8 (1)° for Th and 67.7 (1)° for U. The difference in M–O bond lengths for the uranium complex [0.027 (5) Å] vs. a difference of 0.004 (4) Å in the thorium complex is attributed to a ligand field effect of the  $5f^2$  electronic configuration of U(IV) vs.  $5f^0$  for Th(IV). Green crystals of the uranium complex, obtained from basic aqueous solution, conform to the space group  $I\bar{4}$  with  $a = 14.659$  (3) and  $c = 9.984$  (4) Å. For 3660 independent data with  $F_o^2 > 3\sigma(F_o^2)$  full-matrix least-squares refinement with anisotropic thermal parameters for all nonhydrogen atoms converged to unweighted and weighted  $R$  factors of 3.8 and 4.5%, respectively. The colorless thorium compound, also obtained from basic aqueous solution, has  $a = 14.709$  (4) and  $c = 9.978$  (3) Å. For 5038 independent data refinement as above converged to unweighted and weighted  $R$  factors of 4.3 and 5.3%, respectively.

### Introduction

A continuing project in this laboratory has been the development of powerful chelating agents highly specific for tetravalent actinide ions. One application of such compounds is their use in treating accidental plutonium poisoning. Although treatment procedures have been developed for such poisoning, they are severely hampered by the lack of sequestering agents which are both relatively specific and very strong chelating agents for Pu(IV). Controlled experiments on animals as well as data from industrial accidents show that in mammals plutonium is moved and stored by the iron transport and storage compounds transferrin and ferritin.<sup>2–5</sup> It is this analogy of the chemistry of  $\text{Pu}^{4+}$  to  $\text{Fe}^{3+}$  in biological systems that has been the guiding principle in the design of an actinide sequestering agent. Bacteria have developed very efficient iron sequestering agents for obtaining ferric ion from mammalian hosts.<sup>6</sup> Typically, these siderophores employ three bidentate chelating moieties bound to a trimeric backbone. In particular, the iron transport agent enterobactin employs three catechol (*o*-dihydroxybenzene) ligands to octahedrally coordinate iron.<sup>7</sup> In preparing an actinide-chelating analogue, four catechols are provided to take advantage of the higher coordination number found among these metals as well as to introduce specificity.<sup>1</sup> The complexes formed by actinide(IV) ions and the catecholate dianion, in which the steric restraints of a macrochelate are absent, serve as structural archetypes for designing the optimum actinide(IV) macrochelate. Therefore, as part of a continuing project directed toward the synthesis and characterization of chelating agents specific for actinide ions we report here the structure of tetrakis(catecholato)thorate(IV) and -uranate(IV),  $\text{Na}_4[\text{M}(\text{C}_6\text{H}_4\text{O}_2)_4] \cdot 21\text{H}_2\text{O}$  ( $\text{M} = \text{Th}, \text{U}$ ).

Little is known about the coordination chemistry of catechol with the actinides. There are old reports of isolable compounds with formulas assigned from analytical data alone. These include apparently polymeric materials such as  $\text{K}_2\text{Th}_3(\text{C}_6\text{H}_4\text{O}_2)_7 \cdot 20\text{H}_2\text{O}$  and  $[\text{C}_5\text{H}_5\text{NH}]_2[\text{Th}_2(\text{C}_6\text{H}_4\text{O}_2)_3(\text{OH})_4] \cdot 10\text{H}_2\text{O}$  as well as the presumably monomeric salts,  $[\text{NH}_4]_2[\text{Th}(\text{C}_6\text{H}_4\text{O}_2)_3] \cdot \text{C}_6\text{H}_6\text{O}_2$ ,  $[\text{NH}_4]_2[\text{Th}(\text{C}_6\text{H}_4\text{O}_2)_3] \cdot 5\text{H}_2\text{O}$ , and  $\text{H}_4\text{Th}(\text{C}_6\text{H}_4\text{O}_2)_4$ .<sup>8–11</sup> Similar compounds have been reported for uranium.<sup>12</sup> In addition, solution studies of actinide catecholates led to the conclusion that polymeric compounds were prominent.<sup>13,14</sup> This work, then, reports the first structural information for these materials.

Considering the long and intense interest in actinides for their various applications, it is surprising how little structural information is available for eight-coordinate actinide compounds. For such compounds two limiting geometries are prevalent: square antiprisms ( $D_{4d}$ ) and trigonal-faced dodecahedra ( $D_{2d}$ ).<sup>15</sup> The structure of  $\beta$ -tetrakis(acetylacetonato)uranium(IV) consists of a uranium atom coordinated by eight oxygen atoms in the form of a square antiprism.<sup>16</sup> Trigonal-faced dodecahedral coordination is observed in the Th(salicylaldehydato)<sub>4</sub> complex.<sup>17</sup> The uranium and thorium catecholates reported here have coordination polyhedra which are very close to the idealized trigonal-faced dodecahedron.

### Experimental Section

All experimental manipulations with catechol were carried out under an inert atmosphere free of  $\text{O}_2$  either on a Schlenk line or in a recirculating atmosphere glovebox. Thorium tetrachloride (ROC-RIC), catechol (a generous gift of Crown-Zellerbach Corp.), sodium hydroxide (Mallinckrodt), and uranium tetrachloride (ROC-RIC) were used without further purification. The compounds were characterized using a Perkin-Elmer Model 337 infrared spectrophotom-